Available online www.jsaer.com

Journal of Scientific and Engineering Research, 2024, 11(6):10-17

Research Article

ISSN: 2394-2630
CODEN(USA): JSERBR

Temperature Compensation Method for Resistive Pressure Sensor Based on Random Forest Algorithm

Gao Chenying[1], Zheng Yao[2]

[1]School of business administration, Henan Polytechnic University, Jiaozuo 454000
[2]School of Mechanical and Power Engineering, Henan Polytechnic University, Jiaozuo 454000

Abstract Pressure sensors play a crucial role in various industries, especially in the industrial sector. However, due to their inherent temperature drift characteristics, the measurement results may not be accurate enough, leading to the inability to achieve precise control over equipment and production processes. Therefore, temperature compensation for the measurement results is essential. Commonly used temperature compensation methods include interpolation, BP neural networks, etc., but their calculations are relatively complex. In this paper, we propose a temperature compensation method for pressure sensors based on the random forest algorithm. This algorithm can handle complex data more quickly and accurately. Simulation results demonstrate the effectiveness and reliability of this algorithm.

Keywords Random forest algorithm, Pressure sensor, Temperature compensation, Temperature drift

Introduction

Pressure sensors are widely used in various fields such as transportation, medical, and industrial sectors, and have become indispensable tools for production automation, measurement, scientific testing, and diagnostic systems. The quality of a system is critically dependent on the characteristics of the sensors and the accuracy and reliability of the output information. However, in practical production, sensors often exhibit cross-sensitivity output characteristics and are easily influenced by various environmental factors such as temperature, noise, and power supply fluctuations. The static characteristics of the sensors are not only affected by a single environmental parameter but sometimes even by multiple non-target parameters, leading to unstable sensor performance and low measurement accuracy.

With the development of the integrated circuit and semiconductor industries, different fields have increasingly stringent requirements for the accuracy of pressure sensor transmitters. Silicon piezoresistive pressure sensors utilize the piezoresistive effect of silicon to convert pressure signals into electrical signals. They are characterized by high measurement accuracy, fast dynamic response, high sensitivity, and reliability. Therefore, silicon piezoresistive pressure sensors have been widely used in fields such as rail transportation, aerospace, and petroleum and petrochemical industries. Silicon piezoresistive pressure sensors use a Wheatstone bridge composed of silicon resistors with piezoresistive effects to transmit pressure signals. However, silicon resistor materials are sensitive to temperature, and manufacturing processes have limitations. As a result, silicon piezoresistive sensors exhibit temperature drift. Currently, most scholars eliminate the effects of temperature drift through temperature compensation.

Currently, methods to eliminate the influence of temperature drift can be categorized into hardware compensation and software compensation. Hardware compensation optimizes manufacturing processes, circuit principles, and circuit parameters to compensate for sensor temperature drift. For example, Wang proposed a new control system to reduce the impact of temperature drift. This system can ensure that the maximum measurement error within the pressure range of 100~1100 hPa and the temperature range of -45°C to 45°C does not exceed ±0.2 hPa. M. Aryafar and others proposed a new compensation technique that can reduce the temperature sensitivity coefficient (TCS) of traditional non-compensated sensors to zero. However, hardware compensation is complex, difficult, less reliable, and less accurate. In contrast, software compensation methods, based on techniques such as lookup tables, interpolation, artificial intelligence, and numerical analysis, adjust sensor output signals with high compensation accuracy, low cost, and easy debugging.

Software compensation mainly includes two categories: numerical calculation methods and machine learning methods. Numerical calculation methods such as lookup tables, interpolation, and surface fitting rely on function fitting and interpolation. Traditional numerical calculation methods have advantages such as low computational complexity, good stability, real-time performance, and ease of implementation. Many scholars have conducted in-depth research on this. For example, Lin Zhu et al. used the method of least squares support vector machine to reduce the maximum temperature drift from 8901.4 Pa to 2.0 Pa within the temperature range of -40°C to 70°C and the pressure range of 20 kPa to 260 kPa. Scholars like Liu Peng used numerical analysis method combined with cubic spline interpolation, least squares method, and Newton interpolation method to establish a sensor temperature compensation model. The maximum relative error of this temperature compensation model within the range of -40°C to 80°C is 0.19%.

However, numerical calculation methods are influenced by the accuracy of calibration data and the problem of increasing the order of fitting, so currently, most researchers use machine learning methods for temperature compensation of pressure sensors. For example, Wu Kaifeng used a genetic algorithm (GA) (full-scale relative error is 0.01%FS), Zhu Zhifeng improved the particle swarm optimization algorithm (PSO) (full temperature zone accuracy is 0.1364%), Yin Jiale and others proposed an algorithm based on FOA-LSSVM Fly Optimization Least Square Support Vector Machine (FOA-LSSVM) (the sensitivity temperature coefficient is improved from the compensated α′S=2.505×10-4/℃ to the original α′S=2.03×10-3/℃ by one order of magnitude), and the firefly algorithm (FA) and the gray wolf optimization algorithm (GWO) proposed by Xueliang Z et al. (full-scale error is reduced to 0.03%) and other machine learning methods. These methods determine the temperature compensation amount based on calibration test data and algorithms and can effectively improve temperature compensation accuracy. However, due to the complexity of data processing, a large number of samples, long training time, unstable algorithms, dependence on high-performance computers, and difficulty in loading into MCU chips, the application of these methods in engineering fields is severely constrained.

The random forest algorithm (RF) is a classifier proposed by Leo Breiman and Adele Cutler, which uses multiple trees to train samples and make predictions. RF can be used for data classification and regression prediction, with the characteristics of fast learning speed, ability to handle large sample data, and high accuracy. Currently, it is commonly used in fields such as construction, ecological environment, and finance. For example, Aseel Hussien and Anna Hoła respectively used RF to predict the reliability of building structures and the moisture content of buildings, and Xiaobin Ma and others used RF to predict the ecological restoration of the Yangtze River Delta.

Therefore, this paper models the data of silicon piezoresistive pressure sensors using the random forest algorithm. By analyzing the results of the algorithm, the influence of pressure sensor temperature drift on the actual pressure measurement results can be reduced, enabling more precise control of the production process, timely handling of abnormal production, improving the reliability of pressure prediction for the production system, and consequently enhancing the stability of the production system.

Experimental Object and Data

Silicon Piezoresistive Pressure Sensor

The silicon piezoresistive pressure sensor consists of a silicon piezoresistive pressure sensing core and a signal processing module. The piezoresistive effect of semiconductor materials is used to indicate the pressure changes of the silicon resistive pressure sensing core. The working principle is shown in Figure 2-1, which utilizes four high-precision silicon piezoresistors to form a Wheatstone bridge. The output voltage signal is adjusted by the resistance change caused by tensile and compressive stress, and then the pressure is converted into an electrical signal through the signal conditioning of the operational amplifier.

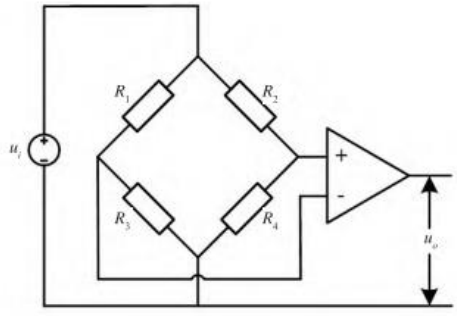

Figure 1: Principle Diagram of Silicon Resistive Pressure Sensor

When the pressure sensor is subjected to pressure stress in a certain direction, according to the piezoresistive effect, the resistance of the silicon piezoresistor will change, thereby affecting the resistance value change in the Wheatstone bridge. According to Kirchhoff's voltage law, we have:

$$\text{Equation (1): } u_0 = ku_i\left(\frac{R_1}{R_1+R_2} - \frac{R_3}{R_3+R_4}\right)$$

Where: u_i is the supply voltage to the Wheatstone bridge; u_0 is the output voltage of the pressure sensor; R1, R2, R3, and R4 are the resistances at different positions in the Wheatstone bridge circuit; k is the amplification factor of the operational amplifier under ideal conditions. In the initial state without pressure input, R1 = R2 = R3 = R4 = R, indicating that the output of the pressure sensor is 0 when not subjected to any pressure. When the sensor is subjected to pressure stress, the resistance values of the four silicon piezoresistors change, causing the bridge to lose its balanced state, which can be expressed as:

$$\text{Equation (2): } u_0 = \frac{u_1}{R}\mathrm{d}R$$

Where: $\mathrm{d}R$ is the change in resistance of the silicon piezoresistor when subjected to pressure stress.
Ideally, if the sensitivity of the silicon resistive pressure sensing core is constant, the output voltage of the bridge would be directly proportional to the pressure. However, the temperature coefficient and the piezoresistive coefficient change with temperature, leading to nonlinearity and temperature drift of the sensor, affecting its sensitivity and accuracy.

Selection of Experimental Data

Due to equipment limitations, the characterization experiment data of DRUCK absolute diffusion silicon piezoresistive pressure sensors are selected as the basic data for this paper. It includes ten temperature preservation processes at ten different temperature points, including -20°C, -10°C, 0°C, 10°C, 20°C, 30°C, 40°C, 50°C, 60°C, and 70°C. This data is derived from the paper "A comprehensive compensation method for piezoresistive pressure sensor based on surface fitting and improved grey wolf algorithm" and is obtained by sampling the output of the pressure sensor under set standard pressure generated by a high-performance automatic pressure calibrator. Specific data is shown in Table 1.

Table 1: Experimental Data of Pressure Input and Output

P (KPa)	T (℃)									
	-20.05	-10.04	0.03	9.96	19.93	30.00	39.94	50.04	59.93	69.97
	VAD									
100	30,308	30,038	29,780	29,496	29,176	28,935	28,612	28,301	27,913	27,628
200	39,069	38,651	38,253	37,834	37,381	37,027	36,588	36,142	35,650	35,253
400	56,615	55,892	55,214	54,523	53,810	53,208	52,525	51,861	51,134	50,514
600	74,188	73,166	72,199	71,234	70,263	69,415	68,494	67,58	66,630	65,789
800	91,789	90,463	89,205	87,968	86,734	85,633	84,467	83,334	82,149	81,082
1000	109,418	107,786	106,237	104,721	103,225	101,890	100,467	99,103	97,679	96,386
1200	127,079	125,132	123,296	121,500	119,741	118,153	116,487	114,883	113,228	111,708
1400	144,763	142,510	140,377	138,299	136,275	134,434	132,527	130,673	128,791	127,045
1600	162,481	159,916	157,482	155,126	152,830	150,734	148,584	146,486	144,371	142,396
1800	180,230	177,345	174,614	171,967	169,412	167,056	164,652	162,316	159,969	157,762
2000	198,008	194,803	191,769	188,842	186,014	183,395	180,750	178,165	175,578	173,148

Based on the experimental data, corresponding line charts can be plotted, as shown in Figure 2, where it can be clearly observed that the output values VAD of the pressure sensor under different pressures undergo significant changes with temperature variation. At a certain pressure, VAD decreases linearly with increasing temperature. However, in the high-pressure range, the influence of temperature on VAD becomes more severe. Therefore, VAD exhibits significant nonlinearity across the entire pressure range. Consequently, the nonlinear effect of temperature on the pressure sensor results in low measurement accuracy, necessitating appropriate temperature compensation. Otherwise, measurement accuracy will be compromised, affecting the monitoring of the entire production system.

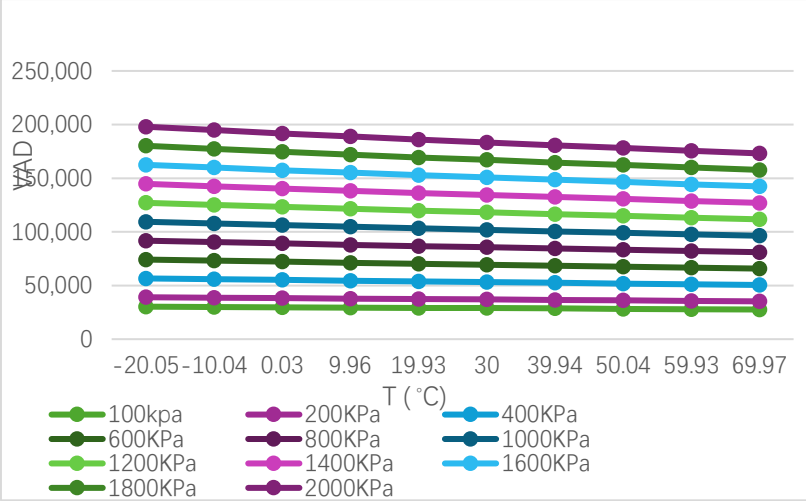

Figure 2: Pressure Output of Pressure Sensor at Different Temperatures

Temperature Compensation Model Based on Random Forest Algorithm (RF)

The random forest algorithm model is a machine learning method that includes multiple decision tree classifiers, proposed by Breiman in 2001. The random forest model has high accuracy and effectiveness in data classification, sample regression, and model prediction, with minimal influence from outliers and noise. It is widely used in medicine, economics, ecology, biology, and geography. The random forest algorithm can train datasets of pressure under different temperatures, obtain corresponding real values through simulation tests, compare them with predicted results, and continuously use machine learning to compensate for pressure under different temperatures, making the measurement results more accurate. In this paper, MATLAB software is used to compensate pressure sensors using a random forest regression prediction model.

Firstly, the data from Table 2 is imported into MATLAB, with different temperatures as the feature variables of the dataset. According to GB/T15487-2015, general performance tests should be conducted at atmospheric temperatures between 18-22°C. Therefore, target values are set at VAD values of 29000, 37000, 53000, 70000, 86000, 102000, 119000, 135000, 151000, 168000, and 185000 for pressures of 100Kpa, 200Kpa, 400Kpa, 600Kpa, 800Kpa, 1000Kpa, 1200Kpa, 1400Kpa, 1600Kpa, 1800Kpa, and 2000Kpa, respectively.

Table 2: Dataset after ±3 of Original Data

Temperature -20.05	Temperature -10.04	Temperature 0.03	Temperature 9.96	Temperature 19.93	temperature 30	Temperature 39.94	Temperature 50.04	Temperature 59.93	Temperature 69.97	target value
30,311	30,041	29,783	29,499	29,179	28,938	28,615	28,304	27,916	27,631	29,000
39,072	38,654	38,256	37,837	37,384	37,030	36,591	36,145	35,653	35,256	37,000
56,618	55,895	55,217	54,526	53,813	53,211	52,528	51,864	51,137	50,517	53,000
74,191	73,169	72,202	71,237	70,266	69,418	68,497	67,586	66,633	65,792	70,000
91,792	90,466	89,208	87,971	86,737	85,636	84,470	83,337	82,152	81,085	86,000
109,421	107,789	106,240	104,724	103,228	101,893	100,470	99,106	97,682	96,389	102,000
127,082	125,135	123,299	121,503	119,744	118,156	116,490	114,886	113,231	111,711	119,000
144,766	142,513	140,380	138,302	136,278	134,437	132,530	130,676	128,794	127,048	135,000
162,484	159,919	157,485	155,129	152,833	150,737	148,587	146,489	144,374	142,399	151,000
180,233	177,348	174,617	171,970	169,415	167,059	164,655	162,319	159,972	157,765	168,000
198,011	194,806	191,772	188,845	186,017	183,398	180,753	178,168	175,581	173,151	185,000
30,305	30,035	29,777	29,493	29,173	28,932	28,609	28,298	27,910	27,625	29,000
39,066	38,648	38,250	37,831	37,378	37,024	36,585	36,139	35,647	35,250	37,000
56,612	55,889	55,211	54,520	53,807	53,205	52,522	51,858	51,131	50,511	53,000
74,185	73,163	72,196	71,231	70,260	69,412	68,491	67,580	66,627	65,786	70,000
91,786	90,460	89,202	87,965	86,731	85,630	84,464	83,331	82,146	81,079	86,000
109,415	107,783	106,234	104,718	103,222	101,887	100,464	99,100	97,676	96,383	102,000
127,076	125,129	123,293	121,497	119,738	118,150	116,484	114,880	113,225	111,705	119,000
144,760	142,507	140,374	138,296	136,272	134,431	132,524	130,670	128,788	127,042	135,000
162,478	159,913	157,479	155,123	152,827	150,731	148,581	146,483	144,368	142,393	151,000
180,227	177,342	174,611	171,964	169,409	167,053	164,649	162,313	159,966	157,759	168,000
198,005	194,800	191,766	188,839	186,011	183,392	180,747	178,162	175,575	173,145	185,000
30,308	30,038	29,780	29,496	29,176	28,935	28,612	28,301	27,913	27,628	29,000
39,069	38,651	38,253	37,834	37,381	37,027	36,588	36,142	35,650	35,253	37,000
56,615	55,892	55,214	54,523	53,810	53,208	52,525	51,861	51,134	50,514	53,000
74,188	73,166	72,199	71,234	70,263	69,415	68,494	67,583	66,630	65,789	70,000
91,789	90,463	89,205	87,968	86,734	85,633	84,467	83,334	82,149	81,082	86,000
109,418	107,786	106,237	104,721	103,225	101,890	100,467	99,103	97,679	96,386	102,000

127,079	125,132	123,296	121,500	119,741	118,153	116,487	114,883	113,228	111,708	119,000
144,763	142,510	140,377	138,299	136,275	134,434	132,527	130,673	128,791	127,045	135,000
162,481	159,916	157,482	155,126	152,830	150,734	148,584	146,486	144,371	142,396	151,000
180,230	177,345	174,614	171,967	169,412	167,056	164,652	162,316	159,969	157,762	168,000
198,008	194,803	191,769	188,842	186,014	183,395	180,750	178,165	175,578	173,148	185,000

Next, the data is divided into training and testing sets. The ±3 data obtained from Table 2 are used as the training set to train the random forest model. The original data from Table 2 is used as the testing set to evaluate the effectiveness of the training. Experimental data (Table 3-1) is obtained. The dataset is shuffled, and the first 22 rows (excluding the feature row) are used as the input data for the training set, with the 11th column of the first 22 rows serving as the output data. The first 10 columns of rows 23-33 are used as the input data for the testing set, with the 11th column of rows 23-33 serving as the output data. Normalization integration is applied to both the training and testing sets, followed by transposition to adapt the normalized data to the model.

The training model is set with 1000 decision trees, with a minimum leaf size of 5 for each tree. Error plots are generated to visualize the error curve and establish the corresponding regression model, as shown in Figure 3.

```
%%  Training model
trees = 100;                                % Number of decision trees
leaf  = 5;                                  % Minimum leaf number
OOBPrediction = 'on';                       % Open error diagram
OOBPredictorImportance = 'on';              % Computational feature importance
Method = 'regression';                      % Classification or regression
net = TreeBagger(trees, p_train, t_train, 'OOBPredictorImportance', OOBPredictorImportance,...
      'Method', Method, 'OOBPrediction', OOBPrediction, 'minleaf', leaf);
importance = net.OOBPermutedPredictorDeltaError;  % importance
```

Figure 3: *Training Model of Random Forest Algorithm*

Through simulation testing of the configured random forest algorithm model and subsequent reverse normalization of the obtained results, corresponding predicted values are obtained.

Temperature Compensation Experiment Analysis The predictive values obtained from the random forest algorithm model are validated through MATLAB simulation, calculating the root mean square error of the model to measure its prediction effectiveness. The following results are obtained through validation:

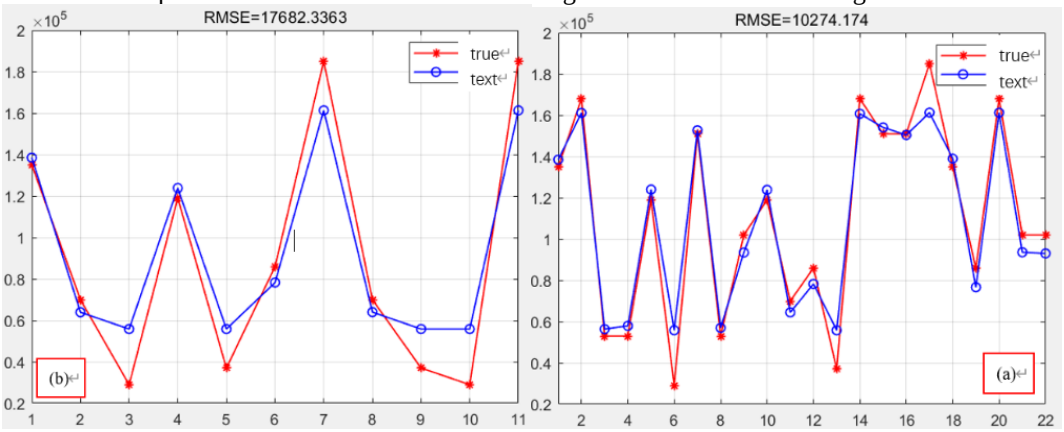

Figure 4: Comparison of Predictive Results between Training (a) and Testing (b) Sets

Predictions of pressure sensor readings are made using the random forest algorithm regression on the training set. From the left center of Figure 4, it can be observed that the fluctuation of actual pressure values measured by the sensor due to temperature is smaller than the fluctuation of predicted values by the model. This indicates that the influence of temperature on the measured values of the pressure sensor is attenuated. Running the model with actual pressure sensor data yields results as shown on the right side of Figure 4, demonstrating that the model remains effective in reducing the impact of temperature on pressure sensors in practical situations, thereby achieving temperature compensation.

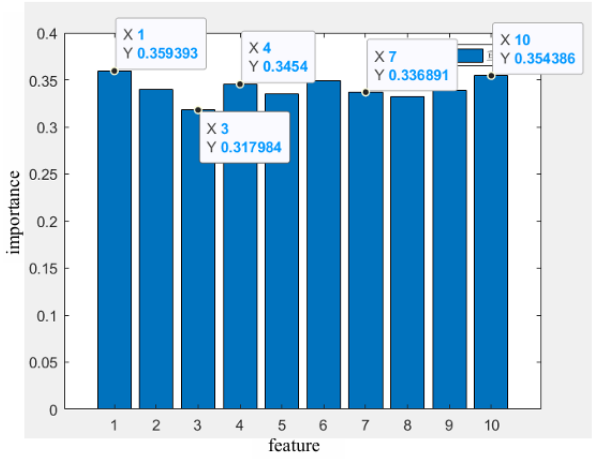

Figure 5: Impact of Different Temperatures on Pressure Sensor

Figure 5 shows the importance of each temperature on the model's predictive effectiveness. Features 1 to 10 represent temperatures from -20°C to 70°C, respectively. It is evident that temperatures at -20°C and 70°C have a higher importance on the pressure sensor, indicating a greater influence on pressure measurements at these temperatures, consistent with the nonlinear nature of temperature drift in pressure sensors, proving the effectiveness of the model.

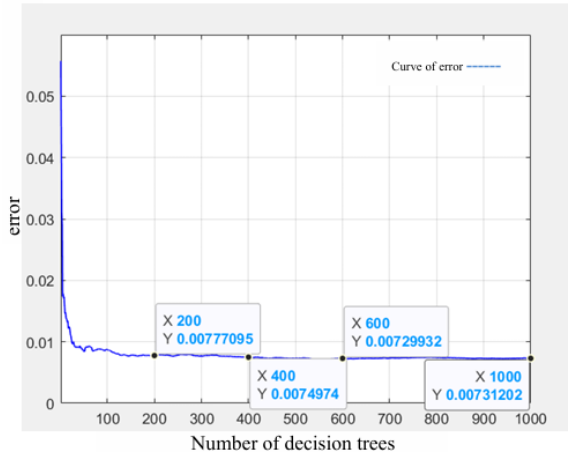

Figure 6: Error Curve of Random Forest Algorithm Model

Subsequently, error estimation is performed on the model, resulting in the error curve shown in Figure 6. It can be observed that as the number of model iterations increases, the error for temperature compensation gradually decreases. When the model runs 1000 times, the final error of the model is only 0.00731, indicating that the model's temperature compensation for pressure sensors is relatively stable, proving the reliability of the model.

Model Validation

To further validate the effectiveness and feasibility of the model, measurements of pressure sensors between 0-5000 Kpa and temperatures between -20°C and 70°C are selected for validation.

Table 3: Calibration Data for 0-5000 Kpa Pressure Sensor

P (KPa)	T (˚C)									
	-20	-10	0	10	20	30	40	50	60	70
	VAD									
0	999.0	999.6	999.9	1000.2	1000.2	1000.6	1003.9	1001.2	1002.5	1005.4
500	1212.8	1209.7	1206.3	1203.3	1200.0	1197.6	1197.9	1192.4	1191.2	1191.7
1000	1426.5	1419.7	1412.6	1403.3	1399.8	1394.5	1391.9	1383.7	1379.9	1377.9
1500	1640.2	1629.7	1618.9	1609.3	1599.7	1591.4	1585.9	1575.0	1568.7	1564.2
2000	1853.8	1839.7	1825.2	1812.3	1799.6	1788.4	1780.0	1766.4	1757.6	1750.5
2500	2068.0	2050.2	2032.0	2015.8	1999.9	1985.8	1974.5	1958.4	1947.2	1938.2
3000	2281.4	2260.0	2238.2	2218.7	2199.7	2182.7	2168.5	2149.7	2136.0	2124.5

3500	2495.5	2470.4	2445.0	2422.2	2400.0	2380.2	2363.1	2341.9	2325.7	2311.8
4000	2709.1	2680.3	2651.3	2625.2	2599.9	2577.1	2557.3	2533.5	2514.5	2498.3
4500	2923.1	2890.7	2858.0	2828.7	2800.1	2774.6	2751.8	2725.5	2704.2	2685.6
5000	3136.5	3100.5	3064.3	3031.6	3000.0	2971.5	2945.8	2917.0	2893.1	2872.0

Applying the data to the random forest algorithm model yields the following results.

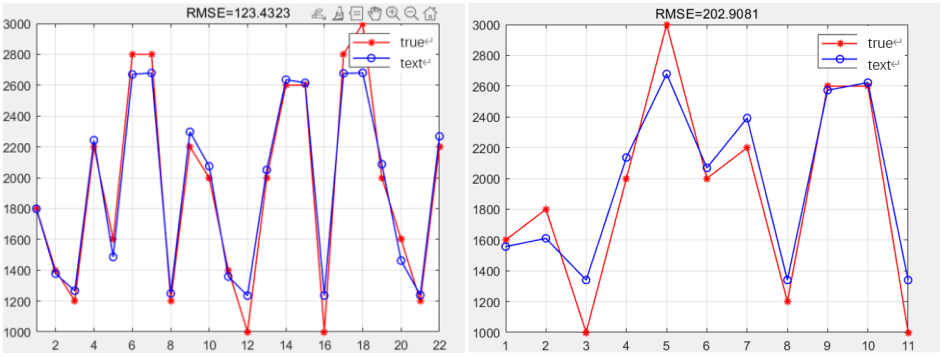

Figure 7: The results of the training (left) set and the test (right) set of the pressure sensor between 0-5000Kpa and -20°C--70°C

By training the data, similar results to Figure 4-1 can be obtained. Regardless of whether it is the training set or the test set, convergence can be achieved for the maximum and minimum values of the data. That is, it is possible to compensate for the measurement results of the resistive pressure sensor under low and high temperature conditions, thereby achieving more accurate monitoring of the entire production system. This further demonstrates the effectiveness of the method.

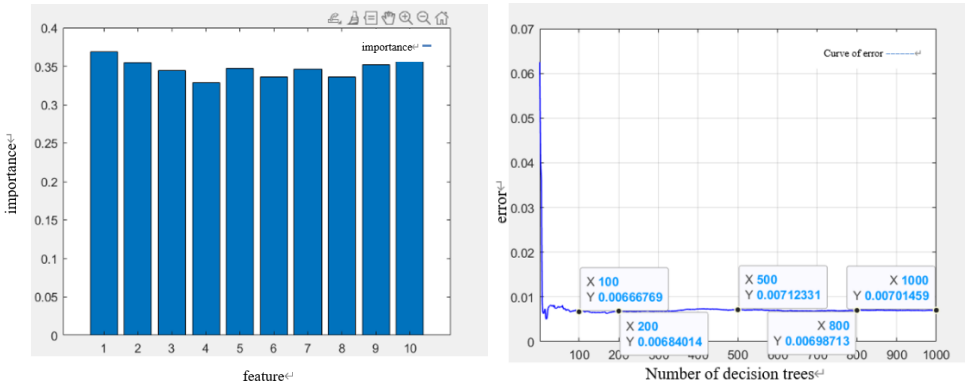

Figure 8: Feature Importance and Model Error Curve

From Figure 5-2, it can be seen that the importance obtained from the data is similar to Figure 4-2, with extreme temperatures having a significant impact on the model's prediction results, and the model's error fluctuating around 0.007.

Conclusion

This study establishes a new temperature compensation model based on the random forest algorithm combined with pressure values at different temperatures. The model can compensate for the temperature of pressure sensor measurements, reducing the influence of temperature on sensor measurement results. Compared to other models, this model has faster learning speed, handles more data, is simpler to operate, and has higher prediction accuracy. It can compensate for pressure at different temperatures, with a measurement error of only 0.00731, significantly improving the accuracy of pressure sensors and having practical value.

By using the random forest algorithm to compensate for the pressure values of resistive pressure sensors at different temperatures, firstly, through the analysis of two sets of experimental data, it is proven that this method is effective. Secondly, the final errors of the two different data sets are close, demonstrating the applicability and stability of the method. Finally, compared with other methods, the biggest advantage of this method is that it tends to be stable after around 100 iterations. Compared to other methods, this method has a faster learning speed and is simpler and quicker to operate, which facilitates faster detection of pressure anomalies in the entire production system and ensures stable operation of the production system.

References

[1]. Zhang X, Cao H, Wen X, et al. Temperature compensation method for pressure sensor based on iterative learning. Railway Locomotive & Carriage, 2023, 43(01): 83-87.

[2]. Liu Z,Du L,Zhao Z, et al. A chip-level oven-controlled system used to improve accuracy of silicon piezoresistive pressure sensor[J]. Measurement,2019,143.

[3]. Aryafar M,Hamedi M,Ganjeh M. A novel temperature compensated piezoresistive pressure sensor[J]. Measurement,2015,63.

[4]. Tian W. FPGA implementation of temperature compensation for pressure sensor based on BP neural network. [Dissertation]. Heilongjiang University, 2020. DOI:10.27123/d.cnki.ghlju.2020.000479.

[5]. Liu H. Research on temperature compensation method of silicon piezoresistive pressure sensor based on artificial neural network. [Dissertation]. Huaibei Normal University, 2020. DOI:10.27699/d.cnki.ghbmt.2020.000197.

[6]. Liu H, Li H. Research on temperature compensation method of pressure sensor based on BP neural network. Journal of Sensor Technology, 2020, 33(05): 688-692+732.

[7]. Qiao W. Temperature compensation of pressure sensor based on BP neural network model. Journal of Huaiyin Normal University (Natural Science Edition), 2019, 18(04): 322-327. DOI:10.16119/j.cnki.issn1671-6876.2019.04.009.

[8]. Chen Q, Zuo F, Lu W. Research on temperature compensation of pressure sensor based on artificial fish swarm BP neural network algorithm. Microcomputer & Its Applications, 2016, 35(09): 27-29+33. DOI:10.19358/j.issn.1674-7720.2016.09.009.

[9]. Wang B, Li H. Temperature compensation of silicon piezoresistive pressure sensor based on cubic spline interpolation. Journal of Sensor Technology, 2015, 28(07): 1003-1007.

[10]. Liang Y. Research on temperature compensation and implementation of pressure sensor. Light Industry Standards and Quality, 2022(05): 72-74. DOI:10.19541/j.cnki.issn1004-4108.2022.05.014.

[11]. Li J, Wang J, He H, et al. Research on temperature compensation o [18]Huang X,Zhang X. Investigating the advanced characteristics of SiC based piezoresistive pressure sensors[J]. Materials Today Communications,2020,25.

[12]. Xueliang Z, Ying C, Guanghua W, et al. A comprehensive compensation method for piezoresistive pressure sensor based on surface fitting and improved grey wolf algorithm. Measurement, 2023, 207.

[13]. Wu K, Zhang L, Kan X, et al. Calibration method for pressure sensor based on improved GA-BP neural network. Foreign Electronic Measurement Technology, 2023, 42(02): 38-44. DOI:10.19652/j.cnki.femt.2204497.

[14]. Basov M. High-sensitivity MEMS pressure sensor utilizing bipolar junction transistor with temperature compensation. Sensors and Actuators: A. Physical, 2020, 303.

[15]. Yenuganti S, Zhang H, Zhang C. Langasite crystal based pressure sensor with temperature compensation. Sensors and Actuators: A. Physical, 2018, 281.

[16]. Yumin Y, Shun L, Junhui H. An ultrasonically catalyzed conductometric metal oxide gas sensor system with machine learning-based ambient temperature compensation. Sensors and Actuators: B. Chemical, 2023, 385.

[17]. Fiorillo A, Critello C, Pullano S. Theory, technology and applications of piezoresistive sensors: A review. Sensors and Actuators: A. Physical, 2018, 281.

[18]. Huang X,Zhang X. Investigating the advanced characteristics of SiC based piezoresistive pressure sensors[J]. Materials Today Communications,2020,25.

[19]. Zhu L,Xie B,Xing Y, et al. A Resonant Pressure Sensor Capable of Temperature Compensation with Least Squares Support Vector Machine[J]. Procedia Engineering,2016,168.

[20]. Liu P, He W, Liu Q, et al. Research on temperature compensation method of pressure sensor based on numerical analysis. Refrigeration & Air Conditioning, 2020, 20(08): 77-80.

[21]. Zhu Z, Zhang H. Research on temperature compensation of pressure sensor based on improved PSO optimized wavelet neural network. Instrument Technique and Sensor, 2022(08): 122-126.

[22]. Xiaobin M,Jinhe Z,Peijia W, et al. Estimating the nonlinear response of landscape patterns to ecological resilience using a random forest algorithm: Evidence from the Yangtze River Delta[J]. Ecological Indicators,2023,153.

[23]. Anna H,Sławomir C. Random forest algorithm and support vector machine for nondestructive assessment of mass moisture content of brick walls in historic buildings[J]. Automation in Construction,2023,149.